Identification of Intermediate Pathways of 4-Hydroxynonenal Metabolism in the Rat

Jacques Alary,[†] Yvette Fernandez,[‡] Laurent Debrauwer,[†] Elisabeth Perdu,[†] and Françoise Guéraud*,[†]

Laboratoire des Xénobiotiques, UMR 1089, INRA-Institut National de la Recherche Agronomique, 180 Chemin de Tournefeuille, BP3, 31931 Toulouse Cedex 9, France, and Laboratoire de Neurobiologie, Plasticité Tissulaire et Métabolisme Énergétique, UMR 5018, CNRS-Institut de Recherche Louis Bugnard−IFR31, CHU Rangueil, Bât L1, 31403 Toulouse Cedex 4, France

Received November 29, 2002

The formation of 4-hydroxy-2-nonenal (HNE) conjugates with glutathione (GSH) by Michael addition and subsequent cleavage to yield the related mercapturic acid (MA) conjugates are a major detoxication process. To characterize the metabolic pathways involved in the formation of urinary HNE−MA conjugates in the rat, the metabolism of HNE−thioethers (HNE−GSH, HNE−MA, and HNE−Cys) by rat liver and kidney cytosolic fractions was investigated. The experimental results showed that HNE−GSH is a good substrate for cytosolic incubations whereas HNE−MA and HNE−Cys are poorly metabolized. About 80% of the urinary MA conjugates originate from the primary and major HNE metabolite, namely, the hemiacetalized HNE−GSH. The direct reduction of HNE−GSH by a cytosolic aldo-keto reductase (NADPH) leads to 1,4-dihydroxynonene−GSH (DHN−GSH) and subsequently to DHN−MA. The direct oxidation of HNE−GSH by aldehyde dehydrogenase $(NAD)^+$ leads to 4-hydroxynonenoic−lactone−GSH, the partial hydrolysis of which occurs at physiological pH and accounts for the corresponding 4-hydroxynonenoic−GSH. Both the spontaneous- and the glutathione *S*-transferases-catalyzed retro-Michael cleavages of HNE−GSH and HNA−lactone−GSH are the source of HNE and HNA−lactone, respectively. This latter compound, with both lipophilic and electrophilic properties, is available for microsomal ω-hydroxylation by cytochrome P450 4A enzymes and conjugation with thiol groups and therefore is the most likely candidate for the formation of ω-hydroxylated HNE−mercapturic acid conjugates excreted in rat urine.

Introduction

HNE[1] is a major aldehydic product resulting from the in vivo lipoperoxidation of membrane and lipoprotein ω-6 unsaturated fatty acids (*1*−*3*). This compound, considered as a "second toxic messenger of oxygen free radicals" is cytotoxic, possibly genotoxic, and responsible for enzyme inactivation (ref *4* and for reviews, see refs *5* and *6*). Its high reactivity is expected to be at least partially responsible for the damages observed in free radical pathology. Nevertheless, this compound can also act as a bioactive molecule in either physiological or pathological conditions such as excessive fibrogenesis in various chronic diseases, inflammatory reactions, or neuronal degeneration and may participate in gene expression regulation, cell signaling, and growth (for recent reviews, see refs *7*−*10*). The main defense system against HNE toxicity is the capability of the cells to inactivate this alkenal by various biotransformation pathways, which are not completely elucidated yet.

When administered in vivo, labeled HNE is rapidly metabolized and mainly excreted into urine (*11*, *12*) as a polar group of free ω-oxidized metabolites from HNA and their MA conjugates and a group of less polar MA thioethers originating from the metabolism of the aldehyde moiety. After iv administration of HNE, these two groups of metabolites accounted for 40−50 and 30% of the injected dose, respectively (*11*). This pattern indicates that both oxidation reactions and GSH conjugation are the main metabolic pathways for HNE metabolization. Moreover, in vitro studies concerning HNE metabolism performed with isolated hepatocytes (*13*, *14*), hepatoma cells (*15*), enterocytes (*16*), erythrocytes (*17*), liver slices (*18*), and perfused organs such as liver, kidney, and heart (*17*, *19*, *20*) suggest that HNA and HNE−GSH account for the major and primary metabolites of HNE. The current study was undertaken in order to (i) give a more precise insight into the different pathways involved in the formation of HNE urinary metabolites, (ii) determine the role of liver and kidney in the biotransformation of this compound, and (iii) tentatively identify the enzymes involved in HNE metabolism. Therefore, the parent HNE−GSH and the two thioether derivatives HNE−Cys and HNE−MA were incubated with rat liver and kidney cytosolic fractions. In addition, HNA−lactone was incubated with rat liver microsomes to investigate the possible implication of ω-hydroxylation, as it was previously shown that microsomal P450 4A isozymes were involved in the metabolization of HNE in mice and that these metabolites originating from ω-oxidation represent a large amount of urinary metabolites (*21*, *22*).

* To whom correspondence should be addressed. Tel: 33(0)561 285 383. Fax: 33(0)561 285 244. E-mail: fgueraud@toulouse.inra.fr.
[†] INRA-Institut National de la Recherche Agronomique.
[‡] CNRS-Institut de Recherche Louis Bugnard−IFR31.

[1] Abbreviations: HNE, 4-hydroxy-2,3-*trans*-nonenal; GSH, glutathione; MA, mercapturic acid; DHN, 1,4-dihydroxynonene; HNA, 4-hydroxynonenoic acid; GST, glutathione *S*-transferase; ESI, electrospray ionization; ADH, alcohol dehydrogenase; ALDH, aldehyde dehydrogenase; AKR, aldo-keto reductase; SPE, solid phase extraction.

10.1021/tx025671k CCC: $25.00
Published on Web 02/07/2003

Materials and Methods

Chemicals. Silicagel 60 TLC plates (0.25 mm, 5 cm × 20 cm) were purchased from Merck (Nogent-sur-Marne, France). Disulfiram, pyrazole, phenobarbital, NADH, NADPH, and GSTs from rat liver (EC 2.5.1.18) were purchased from Sigma (Saint Quentin-Fallavier, France).

All solvents and reagents used for the preparation of buffers and HPLC eluents were of the highest purity grade available from Merck. Ultrapure water from Milli-Q system (Millipore, Saint Quentin en Yvelines, France) was used for HPLC eluent preparation.

HNE, DHN, HNA, DHN−GSH, HNA−MA, HNA−lactone−MA, and DHN−MA were synthesized as previously described (*11*, *23*). HNA−lactone−GSH was synthesized as 9OH-HNA−lactone−MA (*21*), using GSH instead of *N*-acetylcysteine. HNA−lactone was obtained by retro-Michael cleavage of HNA−lactone−GSH catalyzed by GSTs.

[4-^{3}H]HNE (purity >95%; specific activity, 222 GBq/mmol) was synthesized at CEA (Service des Molécules Marquées-CEN, Saclay, France) as diethylacetal, according to the method developed in our laboratory (*24*).

HPLC. The HPLC system consisted of a 420 Kontron pump (Zurich, Switzerland) equipped with a 500 μL loop and a Hypersil ultrabase ODS column (5 μm, 250 mm × 7 mm) from Shandon (Eragny, France) protected by a precolumn (Kromasil C18, 10 μm) and connected to a Gilson 202 fraction collector (Gilson, Villiers-le-Bel, France).

All of the experiments were carried out at room temperature (19−22 °C). The mobile phases were delivered at 2.3 mL/min, and the fractions were collected in 4 tubes/min.

The separation of HNE−GSH metabolites was performed using a two step elution with a mobile phase containing 15% acetonitrile and 85% acetic acid (1%, v/v) for 37.5 min and then a mobile phase containing 30% acetonitrile and 70% water for 22.5 min.

For the separation of HNE−MA and HNE−Cys metabolites, a two step elution was used with a mobile phase containing 20% acetonitrile and 80% acetic acid (1%, v/v) for 45 min and then a mobile phase containing 30% acetonitrile and 70% water for 30 min.

MS. ESI/MS analysis was carried out on a Nermag R-10-10-H single quadrupole instrument (Delsi Nermag Instruments, Argenteuil, France) fitted with an Analytica ESI source (Branford, CT) and on a Finnigan LCQ quadrupole ion trap mass spectrometer equipped with the Finnigan ESI source (Thermo Finnigan, Les Ulis, France). The conditions applied to the Analytica ESI source were as follows: needle, ground potential; surrounding electrode, −2500 V; end plate/nozzle, −3500 V; metallized inlet end of the glass transfer capillary, −4500 V. Those applied to the ESI Finnigan source were as follows: needle, −4500 V; heated transfer capillary, 5−20 V. Structural information was obtained by carrying out MS^n experiments on the LCQ instrument under automatic gain control conditions and using helium as the collision gas. Ion isolation and collision conditions were optimized separately for each metabolite to gain maximal structural information.

GC/MS analysis was performed on a Nermag R-10-10-T single quadrupole instrument coupled to a Delsi DI 200 (Delsi Nermag Instruments) gas chromatograph fitted with a BPX5 (25 m × 0.22 mm × 0.2 μm) capillary column (SGE, Villeneuve Saint Georges, France). The samples were injected in the splitless mode. Helium was used as the carrier gas at a flow rate of 1 mL/min with a back pressure of 0.8 bar. The oven temperature was programmed as follows: 50 °C for 50 s, and then from 50 to 230 °C at 25 °C/min, and from 230 to 270 °C at 5 °C/min. The injector and interface temperature were 270 °C. EI mass spectra were generated at 70 eV with an emission current of 200 μA at a source temperature of 220 °C.

Derivatization for GC/MS Analysis. The dry extracts were methylated by addition of 50 μL of etheral diazomethane. After 30 min at room temperature, the solvent was removed under a nitrogen stream. The residue was then dissolved in a mixture of N,O-bis-trifluoroacetamide/trimethylchlorosilane (Pierce Chemical, Rockford, IL) in a 99:1 ratio and heated at 60 °C for 1 h. The solvent was evaporated at 30 °C under nitrogen stream, and hexane (20 μL) was added to the residue. One microliter of the solution was injected into the gas chromatograph.

Synthesis of HNE−Thioether Conjugates. HNE−GSH and HNE−MA were synthesized by reaction of HNE (0.06 mmol, 0.4 MBq) with L-GSH or *N*-acetyl-L-Cys (0.1 mmol) in 5 mL of 0.1 M sodium phosphate buffer, pH 7.5, at 37 °C overnight. Unreacted HNE was vortex-extracted with 4 × 5 mL dichloromethane, and the aqueous phase was brought to pH 1−2 (1 M H_3PO_4) and applied to a 1 g C18 cartridge (Supelco, Saint Quentin-Fallavier, France). The cartridge was washed with 20 mL of 1% (v/v) acetic acid, dried with a nitrogen stream, and then eluted with 10 mL of methanol. HNE−Cys was synthesized as follows: stoichiometric amounts of racemic HNE (0.06 mmol, 0.4 MBq) and L-Cys were reacted in water (pH 7.5) under N_2 at 37 °C overnight. The reaction mixture was then treated as described for HNE−GSH and HNE−MA. The three thioether conjugates were characterized by ESI/MS^n.

HNE−GSH is present as a cyclic hemiacetal (*25*, *26*), and it is likely that this cyclic structure also occurs in HNE−MA and HNE−Cys. HNE−GSH and HNE−MA conjugates consisted of four HPLC resolved diastereoisomers, while HNE−Cys diastereoisomers remained partially unresolved (results not shown). ^{1}H and ^{13}C NMR showed that each diastereoisomer consisted of a pair of enantiomers.

Radioactivity Determination. The samples (cytosolic supernatants and HPLC fractions) were counted in a model 4330 Packard Tricarb scintillation counter (Packard Instrument Co., Downers Grove, IL) with Ultimagold (Packard) as the scintillation cocktail.

Cytosolic Incubations. Wistar rat liver and kidney cytosols were prepared as previously described (*27*). Protein concentrations were determined by the method of Lowry (*28*). All of the incubations were performed in 25 mL Corex centrifuge tubes in a shaking water bath at 37 °C under nitrogen for 2 h. Control incubations consisted of 0.1 M sodium phosphate buffer (pH 7.5) containing 2.5 mg of liver or kidney cytosolic proteins and the thioether substrate (0.2 μmol, 2 KBq). Some incubations were supplemented with 0.5 μmol NADPH or 0.5 μmol NADH in 0.1 mL of 0.1 M sodium phosphate buffer (pH 7.5). For the incubations performed in the presence of inhibitors, pyrazole or phenobarbital were added at a final concentration of 10 and 1 mM, respectively. The inhibition of ALDH by disulfiram was performed as follows: sodium phosphate buffer containing 2.5 mg of cytosolic proteins (2 mL final volume) was added with 10 μL of a 20 mM disulfiram solution in dimethyl sulfoxide, and the sample was preincubated for 30 min at 37 °C. The resulting sample was then added with the thioether substrate and again with 10 μL of a 20 mM disulfiram solution (giving a final concentration of 0.2 mM disulfiram) and incubated for 2 h at 37 °C.

Analysis of HNE−Thioether Conjugate Metabolites. The cytosolic incubation mixtures were vortex-extracted with 4 mL of dichloromethane and centrifuged (10 000*g* for 5 min). The dichloromethane phase was recovered and filtered on a Separation Phase Filter (Whatman SP1, Whatman, Maidstone, U.K.). This treatment was repeated three times. The combined dichloromethane extracts were concentrated to 1 mL under vacuum at room temperature, and a 20 μL aliquot was counted. The dichloromethane extract was concentrated again to about 100 μL and applied to an activated (120 °C, 20 min) TLC plate, which was developed with toluene/ethyl acetate (80:20). The radioactive spots were detected with a TLC Linear Analyzer LB 2832 (Berthold France, La Garenne Colombes, France) and scraped off. The silica was extracted with dichloromethane or dichloromethane/methanol (90:10), and the analytes were characterized by ESI/MS^n or GC/MS.

The aqueous phase was gassed off with a nitrogen stream to remove dichloromethane traces. The aqueous sample was added with 4 vol of methanol and placed at 0 °C for 15 min to

Table 1. Metabolites Amounts Obtained with Rat Liver and Kidney Cytosolic Fractions with Three Different HNE−Thioethers as Substrate, Expressed as the Percentage of the Substrate Dose[a]

metabolite	proposed identification	identification method	% with liver cytosol	% with kidney cytosol
		HNE−GSH		
aqueous phase				
G1	DHN−Cys	ESI/MS	1.7 ± 0.5	3.4 ± 0.4
G2	HNE−Cys	ESI/MS (*18*)	1.4 ± 0.4	3.7 ± 0.7
G3	DHN−GSH	ESI/MS	6.7 ± 1.5	5.0 ± 0.8
G4	HNE−GSH	ESI/MS (*18*)	22.0 ± 1.5	25.5 ± 4.0
G5	HNA−lactone−Cys	ESI/MS	2.4 ± 0.4	4.6 ± 0.7
G6	HNA−lactone−GSH	ESI/MS	23.9 ± 5.3	25.3 ± 6.6
G7	HNA	GC/MS (methylation and silylation)	3.5 ± 0.8	4.4 ± 1.0
organic phase				
G8 (R_f 0.02)	DHN	GC/MS (silylation)	4.2 ± 0.6	3.5 ± 0.8
G9 (R_f 0.26)	HNE	GC/MS (silylation)	10.2 ± 0.7	7.8 ± 0.9
G10 (R_f 0.52)	HNA−lactone	ESI/MS	11.1 ± 0.8	9.5 ± 1.2
		HNE−MA		
M1	HNE−Cys	ESI/MS (*18*)	7.4 ± 1.8	21.1 ± 2.3
M2	HNA−lactone−GSH	ESI/MS	<2	<2
M3	DHN−MA	ESI/MS	<1	<1
M4, M5	HNE−MA	ESI/MS	81 ± 2.0	63.5 ± 3.8
M6	DHN	comp. with std	<2	<2
M7	HNA	comp. with std	<2	3.3 ± 0.5
M8	HNA−lactone−MA	comp. with std	<2	<2
M9	HNE	GC/MS	3.1 ± 0.8	3.7 ± 0.9
		HNE−Cys		
C1	HNE−Cys	ESI/MS (*18*)	78.5 ± 3.2	77.8 ± 4.3
C2	HNA−lactone−Cys	comp. with std	2.0 ± 1.1	1.8 ± 0.9
C3	HNA−lactone−GSH	comp. with std	<1	<1
C4	DHN	GC/MS	3.3 ± 0.5	3.5 ± 0.6
C5	HNA	GC/MS	4.5 ± 0.9	4.5 ± 1.1
C6	HNE	GC/MS	2.8 ± 0.9	3.2 ± 0.8

[a] The results are the mean of three individual determinations ± SD. For HNE−Cys and HNE−GSH, the fragmentation pattern is indicated in the cited reference.

precipitate proteins and then centrifuged (10 000*g* for 10 min). The supernatant was evaporated under vacuum at 45 °C to about 1 mL, diluted to 10 mL with distilled water, and brought to pH 1−2 with 1 M H_3PO_4 (200 μL). The resulting sample was loaded onto a 360 mg C18 Sep Pak Plus cartridge preconditioned with 5 mL of methanol and 10 mL of 1% (v/v) acetic acid. The cartridge was washed with 10 mL of 1% (v/v) acetic acid, dried under a nitrogen stream, and eluted with 5 mL of methanol. The eluate was evaporated to dryness under vacuum at 45 °C and the residue, redissolved in 450 μL eluent, was analyzed by HPLC. The radioactive protein pellet was dissolved in 1 mL of 0.2 M NaOH and directly counted. Preliminary experiments showed that the amounts of dichloromethane extractable metabolites formed with HNE−MA and HNE−Cys as substrates were very low; therefore, the extraction step was deleted for these substrates. The incubation mixture was directly loaded on the C18 cartridge, and the resulting methanolic eluate was evaporated to dryness under vacuum at room temperature and analyzed by HPLC.

Results

A. In Vitro Metabolism of HNE−Thioether Conjugates. After incubation of rat liver or kidney cytosolic fractions, the three different HNE−thioethers substrates were partially metabolized (Table 1). Radio-HPLC chromatograms of HNE−GSH and HNE−MA metabolites are shown in Figures 1 and 2, respectively. The radio-HPLC chromatogram of HNE−Cys metabolites (not shown) was qualitatively identical to that of HNE−MA. About 2% of the starting radioactive dose remained in the protein pellet. The structure of the different metabolites was obtained by mass spectrometry or by comparison with authentic standards (Table 1).

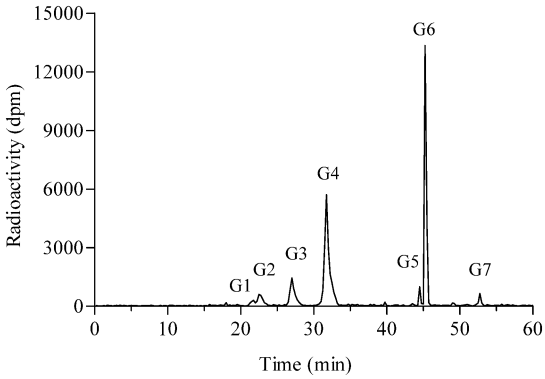

Figure 1. Typical radio-HPLC profile of [4-^{3}H]HNE−GSH nonextractable metabolites from incubation with rat liver cytosol as described in the Material and Methods section.

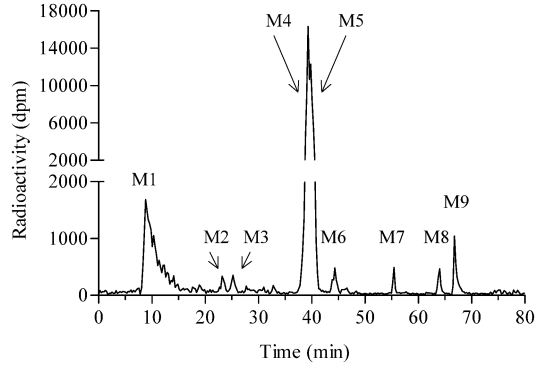

Figure 2. Typical radio-HPLC profile of [4-^{3}H]HNE−MA metabolites from incubation with rat kidney cytosol as described in the Material and Methods section.

Table 2. ESI/MS^n and GC/MS Fragments Ions Observed for HNE−Thioether Metabolites Obtained from Rat Liver and Kidney Cytosolic Fractions and for ω-Hydroxylated HNA−Lactone Obtained with Rat Liver Microsomal Fraction[a]

	ESI/MS^1 *m/z*	ESI/MS^2 *m/z* interpretation	ESI/MS^3 *m/z* interpretation	proposed structure
G1	**280** $[M + H]^+$	**262** $[DHN-Cys + H - H_2O]^+$	244 $[DHN-Cys + H - 2H_2O]^+$ 122 $[Cys + H]^+$ 141 $[DHN + H - H_2O]^+$	DHN−Cys
G3	**466** $[M + H]^+$	448 $[DHN-GSH + H - H_2O]^+$ 319 $[DHN-GSH + H -$ glutamic acid$]^+$		DHN−GSH
G5	**276** $[M + H]^+$	258 $[HNA-lactone-Cys + H - H_2O]^+$ 122 $[Cys + H]^+$ 155 $[HNA-lactone + H]^+$		HNA−lactone−Cys
G6 M2	**460** $[M - H]^-$	442 $[HNA-lactone-GSH - H - H_2O]^-$ 306 $[GSH - H]^-$		HNA−lactone−GSH
G10	**155** $[M + H]^+$	137 $[HNA-lactone + H - H_2O]^+$ **109** $[CH_3-CH_2-CH_2-CH_2-CH=CH-CH=CH]^+$	81 $[CH_3-CH_2-CH=CH-CH=CH]^+$ 67 $[CH_3-CH=CH-CH=CH]^+$	HNA−lactone (Figure 3)
S	**171** $[M + H]^+$	153 $[MH - H_2O]^+$ 125 $[HOCH_2-CH_2-CH_2-CH_2-CH=CH-CH=CH]^+$		9-hydroxy-HNA−lactone

	GC/MS *m/z* interpretation	proposed structure
G7	243 $[M - CH_3]^+$ 227 $[M - CH_3O]^+$ 199 $[M - CH_3 - CO_2]^+$ 187 $[(CH_3)_3-Si-O-CH=CH-COOCH_3]^+$	HNA
G8	287 $[M - CH_3]^+$ 231 $[(CH_3)_3-Si-O-CH-CH=CH-CH_2-O-Si-(CH_3)_3]^+$ 173 $[CH_3-(CH_2)_4-CHO-Si-(CH_3)_3]^+$199 $[M - CH_2$-O−Si−$(CH_3)_3]^+$ 147 $[(CH_3)_2-Si-O-Si-(CH_3)_3]^+$	DHN
G9	228 $[M]^{+\bullet}$ 213 $[M - CH_3]^+$ 199 $[M - CHO]^+$ 184 $[M - CH_3-CHO]^{+\bullet}$ 157 $[(CH_3)_3-Si-O-CH-CH=CH-CHO]^+$	HNE

[a] Metabolites in the first column are named as described in Table 1. Metabolite S is the metabolite obtained during the incubation of HNA−lactone with rat liver microsomal fraction. Bold *m/z* ions indicate the selected ion for further fragmentation.

The characterization of metabolites was performed by ESI/MS or GC/MS analysis (Table 1), and fragmentation patterns are given in Table 2.

To confirm the structures, the fragmentation was compared to that of an authentic standard. Because of the low available amounts of metabolites obtained with HNE−Cys and HNE−MA as substrates, most of these metabolites were characterized only by comparison of their retention time with those of authentic synthesized standards, and a confirmation of the structure by ESI/MS^n was performed only when required.

As no authentic standard of HNA−lactone was available for the comparison of metabolite G10 fragmentation pattern (Figure 3) and as Mw 154 could also correspond to that of 4-oxo-nonenal, a possible metabolite of HNE, additional investigations were performed to unambiguously characterize this metabolite. No hydrazone formation occurred when metabolite G10 was reacted with 2,4-dinitrophenylhydrazine in acidic medium, in contrast to what occurs with 4-oxo-nonenal. Moreover, hydrolysis of G10 (0.1 M Na_2HPO_4, pH 8.9, 5 h, 25 °C) afforded 46% HNA. This chemical behavior together with the fragmentation pattern unambiguously characterize metabolite G10 as HNA−lactone.

To clarify metabolic pathways, additional incubations were performed in the presence of inhibitor or added cofactor. The more relevant experimental results are summarized below.

A.1. Formation of DHN−GSH from HNE−GSH. Incubations performed with HNE−GSH and rat liver and kidney cytosolic fractions in the presence of 10 mM pyrazole, a potent inhibitor of ADH, or in the presence of added NADH cofactor did not modify the formation of DHN−GSH as compared to that of control incubations. The addition of 0.5 μmol of NADPH increased DHN−GSH levels when compared to those obtained in control incubations: 15 vs 6.7% and 11 vs 5% with liver and kidney cytosolic fractions, respectively. Incubations performed in the presence of 1 mM phenobarbital resulted in a 40% inhibition of the HNE−GSH reduction.

A.2. Formation of Oxidized Metabolites. A.2.1. Formation of HNA−Lactone−GSH from HNE−GSH. Cytosolic incubations performed with HNE−GSH as substrate in the presence 0.2 mM disulfiram, a potent ALDH (NAD^+-dependent) inhibitor gave a 95% depletion of the HNA−lactone−GSH formation, as compared to control incubations.

A.2.2. Formation of HNA−Lactone from HNA−Lactone−GSH. Incubation of HNA−lactone−GSH standard with liver cytosolic fraction, for 2 h at 37 °C and pH 7.5, afforded HNA−lactone at about 10% of the HNA−lactone−GSH dose.

A.2.3. Formation of HNA−Lactone−GSH from HNA−Lactone. Incubations of HNA−lactone (2 h, 37 °C, pH 7.5) with GSH, with or without GSTs, afforded 85% of HNA−lactone−GSH.

A.2.4. Formation of HNA−Lactone from HNA. When HNA was placed in mild acid conditions (0.05 M H_2PO_4, 37 °C, overnight), no HNA−lactone formation occurred, while in the same conditions, 4-hydroxy-nonanoic acid spontaneously lactonized.

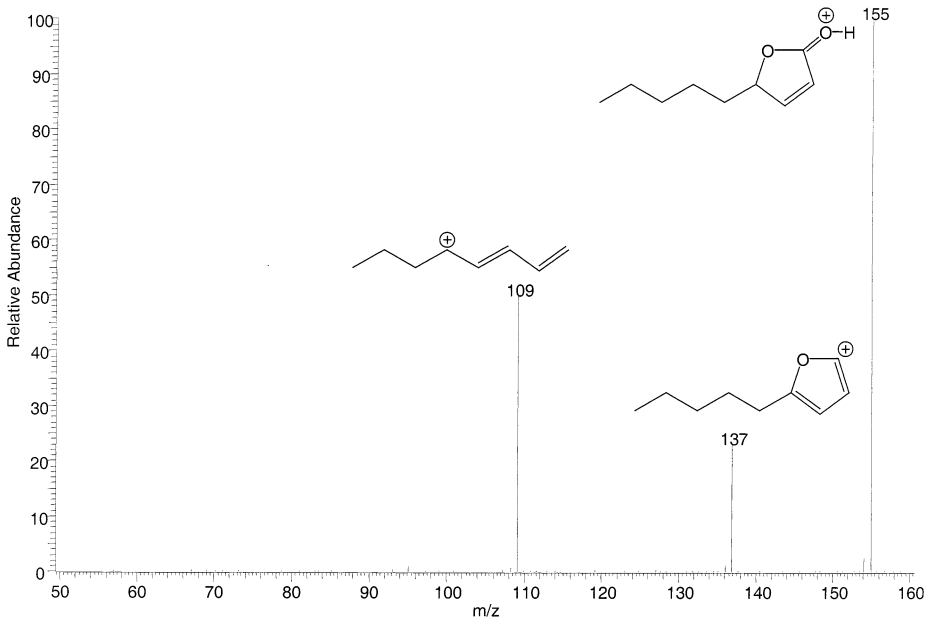

Figure 3. Positive ESI/MS/MS product ion mass spectrum of metabolite G10, the lactone of HNA.

A.2.5. Formation of HNA−Lactone−Cys from HNA−Lactone−GSH or HNE−Cys. Cytosolic incubations performed with HNA−lactone−GSH as substrate gave small amounts of HNA−lactone−Cys. With HNE−Cys standard as substrate in the same conditions, low amounts of HNA−lactone−Cys were also formed.

A.2.6. Origin of HNA−Lactone−MA and HNA−Lactone−GSH from HNA−MA and HNA−GSH, Respectively. In mild acid conditions (1 h, 20 °C, pH 2), the spontaneous lactonization of the two carboxylic acid conjugates occurred with an 80% yield.

A.2.7. Hydrolysis of HNA−Lactone−GSH, HNA−Lactone−MA, and HNA−Lactone. In physiological conditions (37 °C, pH 7.5, 24 h), HNA−lactone−GSH and HNA−lactone−MA afforded 30% of HNA−GSH and HNA−MA, respectively. In the same conditions, HNA−lactone was completely resistant to hydrolysis.

A.3. Retro-Michael Cleavage of HNE−Thioethers. Spontaneous retro-Michael cleavage of HNE−GSH performed in sodium phosphate buffer (2 h, 37 °C, pH 7.5) afforded 2.2% of HNE. The same incubation carried out for 1 h in the presence of 5 units of purified rat liver GSTs afforded increased HNE levels accounting for 9.3% of the thioether dose. Spontaneous retro-Michael cleavage also occurred when HNE−MA or HNE−Cys standards were incubated at 37 °C (pH 7.5) for 2 h, yielding 2.5 and 10% HNE, respectively.

B. ω-Hydroxylation of HNA−Lactone. To give insight into the metabolic pathways involved in the formation of ω-hydroxylated MA conjugates previously evidenced in rat urine (*21*), HNA−lactone (50 nmol) was incubated for 2 h at 37 °C and pH 7.5 with rat liver microsomes (3 mg proteins) and afforded (20% yield) a compound (S) more polar than HNA−lactone, which was characterized by ESI/MS^n as 9-hydroxy-HNA−lactone (Table 2).

Discussion

The current experimental study provides evidence that rat liver and kidney cytosolic fractions are effective in further metabolizing the primary and major HNE metabolite, namely, HNE−GSH, at the HNE hemiacetal moiety. In contrast, HNE−Cys and HNE−MA, which are secondary metabolites of HNE−GSH, were poorly metabolized at the C_9 chain moiety by these cytosolic fractions. The only important metabolization of these two substrates concerns the GSH moiety: HNE−Cys, which originates from *N*-deacetylation of HNE−MA, was formed in large amounts with kidney cytosolic fractions due to the higher activity of cytosolic *N*-deacetylases in this organ as compared to the liver (*29*, *30*).

These results are consistent with the following in vivo results. First, after HNE injection, HNE−MA originating from HNE−GSH only accounted for trace amounts in rat urine (*11*). Second, in rats injected iv with [^{3}H]HNE−MA, 47% of the unchanged compound was excreted in the urine (unpublished result). Moreover, it is likely that the results of our in vitro study underestimate the capacity of HNE−GSH to be metabolized by redox reactions, because of the lack of cofactors (NADPH, NAD^+) in control incubations.

DHN−MA, the Major Urinary HNE Metabolite Originates from HNE−GSH. DHN−MA, which is present in urine of untreated rats and humans (*31*), was proposed as a noninvasive biomarker of in vivo lipid peroxidation (*11*, *12*). It appears to be of primary importance to experimentally investigate its formation pathways from HNE. DHN−MA originates from DHN−GSH, and this conversion involves γ-glutamyltranspeptidase, cysteinyl-glycine dipeptidase, and *N*-acetyltransferases. The activity of the first two enzymes is considered to be lower in rat liver, as compared to kidney (*32*, *33*). Moreover, these enzymes are membrane-bound and their presence in the cytosolic fractions most likely results from a slight contamination during the preparation of these subcellular fractions. The results concerning the low amount of HNE−Cys as a metabolite of HNE−GSH (Table 1) are consistent with the proposed origin of HNE−Cys.

In the cytosolic incubations performed with HNE−GSH as substrate, the major compound resulting from

reductive metabolism was DHN−GSH that reached about 6% of the incubated dose. Because of the absence of a polarized double bond in DHN, which precludes direct Michael addition of GSH to DHN, several authors (*12*, *17*, *23*) proposed that the formation of DHN−GSH should result from the direct reduction of HNE−GSH. Our supplementary experiments in the presence of specific inhibitor or cofactor clearly showed that NADH-dependent ADH was not involved in the reduction of HNE−GSH to DHN−GSH. In contrast, incubations supplemented with NADPH as reductive cofactor and phenobarbital as inhibitor showed that the enzyme(s) involved in this reduction is cytosolic, NADPH-dependent, and phenobarbital-inhibited, three properties that correspond to aldose reductase, which belongs to the AKR superfamily. Indeed, this enzyme purified from bovine lens has been shown to reduce HNE and HNE−GSH to DHN and DHN−GSH, respectively (*34*). This enzyme has also been recently implicated in the reduction of HNE−GSH to DHN−GSH in aortic endothelial cells (*35*) and was shown to be more effective in reducing glutathiolated aldehydes than the related free aldehydes (*36*). However, other data showed that this enzyme is not well-expressed neither in rat nor in human liver (*37*, *38*). Nevertheless, the current results clearly characterize DHN−GSH as a metabolite of HNE−GSH when using rat liver cytosolic preparations, and DHN−MA was formally characterized in human urine (*31*). As aldose reductase and the other members of the AKR superfamily share multiple common properties and overlapping substrate specificites and in the absence of unquestionable data, it must be borne in mind that AKR(s) should be involved in the reduction of HNE−GSH to DHN−GSH. Moreover, it was shown that HNE could induce the expression of another member of the AKR superfamily, namely, aldehyde reductase gene, in rat aortic smooth muscle cells (*39*). Recently, it was also shown that AKR1C1, a human liver AKR, could reduce HNE to DHN with even higher efficiency than human liver aldehyde reductase (AKR1A1) (*40*). However, the efficiency of these enzymes toward HNE−GSH remains to be established.

All Oxidized Mercapturate Derivatives of HNE Originate from the Direct Oxidation of HNE−GSH. In a previous work, we showed that HNA−MA and HNA−lactone−MA were the main MA derivatives from oxidative metabolism of HNE administered in vivo (*11*). At that time, it was suspected that HNA−lactone−MA was formed by the lactonization of HNA−MA following the exogenous mild acidification (1 h, 20 °C, pH 2) required for SPE/HPLC procedures (*21*). In such experimental conditions, chemical lactonization of HNA−GSH standard afforded only 80% of HNA−lactone−GSH. However, in the current study with HNE−GSH as the substrate incubated with cytosolic fractions, no HNA−GSH was found whereas HNA−lactone−GSH accounted for more than 20% of the radioactive starting dose, suggesting that HNA−lactone−GSH should be formed by an endogenous metabolic pathway. However, at physiological pH, the lactonization of HNA−GSH cannot occur since the COOH group of HNA−GSH is in the carboxylate form. These two points preclude any endogenous or exogenous formation of HNA−lactone−GSH from HNA−GSH. Although HNA is present in the control incubations with HNE−GSH as substrate, we cannot hypothesize the formation of HNA−lactone−GSH from HNA since HNA cannot lactonize, even in mild acid conditions because of the presence of the double bond, and cannot be conjugated with GSH, due to the negative charge of the carboxylate at physiological pH. The most likely possibility of HNA−lactone−GSH formation is the direct oxidation of the CHOH group of the cyclic hemiacetal of HNE−GSH to the corresponding oxo group by cytosolic ALDH (NAD^+) leading to the formation of the lactone group, as confirmed by the additional experiments carried out in the presence of disulfiram, a potent ALDH inhibitor. This pathway is strongly supported by the presence of HNA−lactone−GSH in the complete absence of HNA−GSH. This previous formation of the lactone ring implies that the eventual corresponding carboxylic compound originates from the physiological hydrolysis of the lactone ring at pH 7.5.

We show here that HNA−lactone, which is present in our incubations in relatively high amounts, could be at the origin of the polar conjugates found in vivo in the urine of rats administered with HNE (*21*). Indeed, rat liver microsomal incubations carried out with HNA−lactone as substrate show that this compound was ω-hydroxylated. The capacity of HNA−lactone to undergo ω-hydroxylation and the presence in the molecule of polarizable conjugated double bonds required for a conjugation reaction make this compound the most likely candidate for the formation of ω-hydroxylated conjugates.

HNE and HNA−Lactone Thioethers Release the Parent Compounds by Retro-Michael Cleavage. Free metabolites of HNE−thioether derivatives, namely, HNE, DHN, HNA, and HNA−lactone, were found in the cytosolic incubations with the three HNE−thioethers. Because of the presence of two conjugated double bonds, HNE and HNA−lactone account for soft electrophiles, which give spontaneous Michael addition with thiol compounds and a GST-catalyzed conjugation with GSH. The occurrence of this spontaneous forward reaction implies that of the reverse reaction. On the contrary, because DHN and HNA are not electrophilic compounds, neither the forward addition nor the reverse reaction occurs. With HNE−GSH (HNA−lactone−GSH not tested) as the substrate, our in vitro study showed that the retro-Michael reaction was GST-catalyzed, a finding consistent with other GSH conjugates (*41*−*43*). Subsequently, the HNE formed by retro-Michael cleavage undergoes direct redox reactions, which accounts for the formation of DHN and HNA.

The electrophilic compounds HNE and HNA−lactone are exported from the cell and transported elsewhere as thioether conjugates, which can release the active parent compound in physiological conditions. However, in vivo, the retro-Michael cleavage should occur at a low extent, since (i) the GST-catalyzed cleavage of GSH conjugates proceeds intracellularly, where both GSTs and a high level of GSH are localized; (ii) the ratio of the formation/cleavage of GSH conjugates is severalfold in favor of the former reaction in physiological conditions, and it can be expected that the levels of free compounds originating from retro-Michael cleavage should remain very low, especially in the case of HNE and HNA−lactone for which the cyclic form of the conjugate stabilizes the structure (*44*); (iii) in vivo, it can be anticipated that the two major sources of HNE by retro-Michael cleavage, namely, HNE−GSH and HNE−Cys, are readily transformed into HNE−MA, which is a poor substrate for retro-Michael cleavage and is readily excreted in urine;

Scheme 1. Proposed Metabolic Pathways for the Formation of HNE−GSH Metabolites in Rat Liver and Kidney Cytosolic Fractions (Continuous Line Arrows) and Subsequent In Vivo Reactions (Dotted Arrows)

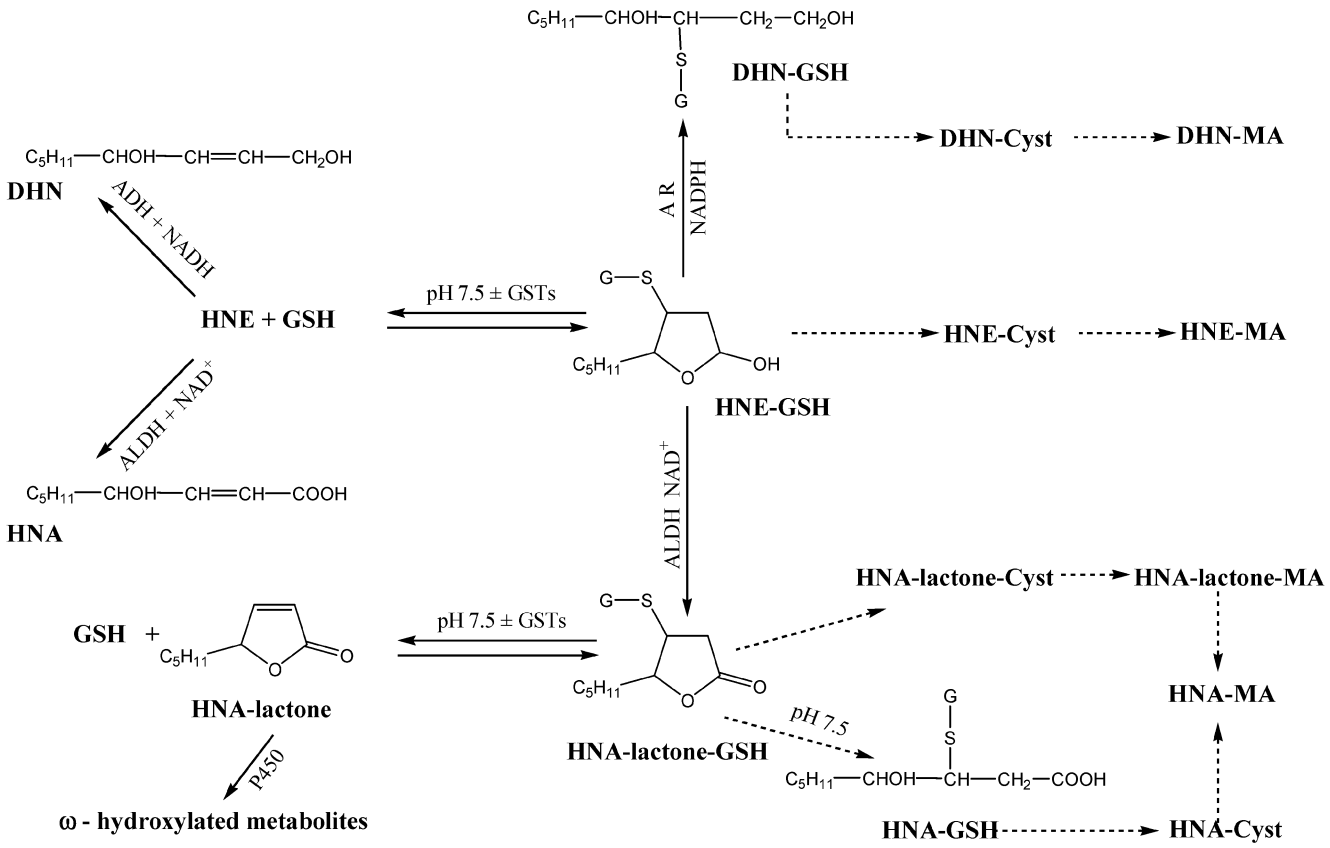

(iv) the fast redox metabolism of HNE−GSH removes the unique source of formation of HNE via the retro-Michael reaction. Therefore, with HNE as aglycone, it could be expected that the release should be low. However, in vivo metabolism study of HNE−GSH or HNE−Cys should be undertaken in order to get a more precise insight of the physiological importance of retro-Michael cleavage of HNE−thioethers, which could serve as transport forms because of their low reactivity with other molecules and could increase the half-life of HNE, as it is the case for other GSH conjugates (*45*, *46*). These transport forms could then release the "free active forms" elsewhere, possibly far away from where they were generated, as it was anticipated by Eisenbrand and co-workers (*47*) for 2-alkenals.

The current study experimentally points out the mechanisms involved in the formation of the major rat urinary HNE metabolites. Since they were formed, HNE−MA and HNE−Cys were shown to be poor substrates for redox reactions; thus, HNE−GSH unquestionably accounts for DHN−MA and HNA−lactone−MA formation. Scheme 1 summarizes the experimentally revealed metabolic pathways that occur in rat liver and kidney cytosols. In the meantime, we have observed that some of the metabolic pathways show stereospecificity (results not shown). This stereospecificity of HNE metabolism could be of physiological importance and is now under investigation.

Acknowledgment. We thank Drs. G. Bories and J. P. Cravedi for reviewing the manuscript.

References

(1) Esterbauer, H. (1982) Aldehydic products of lipid peroxidation. in *Free Radicals, Lipid Peroxidation and Cancer* (McBrien, D. C. H., and Slater, T. F., Eds.) pp 101−128, Academic Press, London.

(2) Esterbauer, H., Zollner, H., and Schaur, R. J. (1990) Aldehydes formed by lipid peroxidation; mechanisms of formation, occurrence and determination. in *Membrane Lipid Oxidation* (Vigo-Pelfrey, C., Ed.) Vol. I, pp 239−283, CRC Press, Boca Raton, FL.

(3) Esterbauer, H., Jürgens, G., Quehenberger, O., and Koller, E. (1987) Autoxidation of human low-density lipoprotein: loss of polyunsaturated fatty acids and vitamin E and generation of aldehydes. *J. Lipid Res.* **28**, 495−509.

(4) Eckl, P. M., Ortner, A., and Esterbauer, H. (1993) Genotoxic properties of 4-hydroxyalkenals and analogous aldehydes. *Mutat. Res.* **290**, 183−192.

(5) Esterbauer, H., Schaur, R. J., and Zollner, H. (1991) Chemistry and biochemistry of 4-hydroxynonenal, malonaldehyde and related aldehydes. *Free Radical Biol. Med.* **11**, 81−128.

(6) Esterbauer, H. (1993) Cytotoxicity and genotoxicity of lipid-oxidation products. *Am. J. Clin. Nutr.* **57** (Suppl.), 779S−786S.

(7) Dianzani, M. U., Barrera, G., and Parola, M. (1999) 4-Hydroxy-2,3-nonenal as a signal for cell function and differentiation. *Acta Biochim. Pol.* **46**, 61−75.

(8) Parola, M., Bellomo, G., Robino, G., Barrera, G., and Dianzani, M. U. (1999) 4-Hydroxynonenal as a biological signal: molecular basis and pathophysiological implications. *Antioxid. Redox Signaling* **1**, 255−284.

(9) Leonarduzzi, G., Arkan, M. C., Başağa, H., Chiarpotto, H., Sevanian, A., and Poli, G. (2000) Lipid oxidation products in cell signaling. *Free Radical Biol. Med.* **28**, 1370−1378.

(10) Poli, G., and Schaur, R. J. (2000) 4-Hydroxynonenal in the pathomechanisms of oxidative stress. *IUBMB Life* **50**, 315−321.

(11) Alary, J., Bravais, F., Cravedi, J. P., Debrauwer, L., Rao, D., and Bories, G. (1995) Mercapturic acid conjugates as urinary end metabolites of the lipid peroxidation product 4-hydroxy-nonenal in the rat. *Chem. Res. Toxicol.* **8**, 34−39.

(12) De Zwart, L. L., Hermanns, R. C. A., Meerman, J. H. N., Commandeur, J. N. M., and Vermeulen, N. P. E. (1996) Disposition in rat of [2-^{3}H]-*trans*-4-hydroxy-2,3-nonenal, a product of lipid peroxidation. *Xenobiotica* **26**, 1087−1100.
(13) Hartley, D. P., Ruth, J. A., and Petersen, D. R. (1995) The hepatocellular metabolism of 4-hydroxynonenal by alcohol dehydrogenase, aldehyde dehydrogenase and glutathione *S*-transferase. *Arch. Biochem. Biophys.* **316**, 197−215.
(14) Siems, W. G., Zollner, H., Grune, T., and Esterbauer, H. (1997) Metabolic fate of 4-hydroxynonenal in hepatocytes: 1,4-dihydroxynonene is not the main product. *J. Lipid Res.* **38**, 612−622.
(15) Tjalkens, R. B., Cook, L. W., and Petersen, D. R. (1999) Formation and export of the glutathione conjugate of 4-hydroxy-2,3-nonenal (4-HNE) in hepatoma cells. *Arch. Biochem. Biophys.* **361**, 113−119.
(16) Grune, T., Siems, W., Kowalewski, J., Zollner, H., and Esterbauer, H. (1991) Identification of metabolic pathways of the lipid peroxidation product 4-hydroxynonenal by enterocytes of rat small intestine. *Biochem. Int.* **25**, 963−971.
(17) Boon, P. J. M., Marinho, H. S., Oosting, R., and Mulder, G. J. (1999) Glutathione conjugation of 4-hydroxy-*trans*-2,3-nonenal in the rat in vivo, the isolated perfused liver and erythrocytes. *Toxicol. Appl. Pharmacol.* **159**, 214−223.
(18) Laurent, A., Perdu-Durand, E., Alary, J., Debrauwer, L., and Cravedi, J. P. (2000) Metabolism of 4-hydroxynonenal, a cytotoxic product of lipid peroxidation, in rat precision-cut liver slices. *Toxicol. Lett.* **114**, 203−214.
(19) Grune, T., Siems, W. G., and Petras, T. (1997) Identification of metabolic pathways of the lipid peroxidation product 4-hydroxynonenal in in situ perfused rat kidney. *J. Lipid Res.* **38**, 1660−1665.
(20) Ishikawa, T., Esterbauer, H., and Sies, H. (1986) Role of cardiac glutathione transferase and of the glutathione S-conjugate export system in the biotransformation of 4-hydroxynonenal in the heart. *J. Biol. Chem.* **261**, 1576−1581.
(21) Alary, J., Debrauwer, L., Fernandez, Y., Paris, A., Cravedi, J. P., Dolo, L., Rao, D., and Bories, G. (1998) Identification of novel urinary metabolites of the lipid peroxidation product 4-hydroxy-2-nonenal in rats. *Chem. Res. Toxicol.* **11**, 1368−1376.
(22) Guéraud, F., Alary, J., Costet, P., Debrauwer, L., Dolo, L., Pineau, T., and Paris, A. (1999) In vivo involvement of cytochrome P450 4A family in the oxidative metabolism of the lipid peroxidation product *trans*-4-hydroxy-2-nonenal, using PPARα-deficient mice. *J. Lipid Res.* **40**, 152−159.
(23) Laurent, A., Alary, J., Debrauwer, L., and Cravedi, J. P. (1999) Analysis in the rat of 4-hydroxynonenal metabolites excreted in bile: evidence of enterohepatic circulation of these byproducts of lipid peroxidation. *Chem. Res. Toxicol.* **12**, 887−894.
(24) Bravais, F., Rao, D., Alary, J., Rao, R. C., Debrauwer, L., and Bories, G. (1994) Synthesis of 4-hydroxy[4-^{3}H]-2(E)-nonen-1-al-diethylacetal. *J. Labeled Compd. Radiopharm.* **36**, 471−477.
(25) Schauenstein, E., Dorner, F., and Sonnenbichler, J. (1968) Uber die Bindung von 4-hydroxy-2,3-enalen an proteinSH-grupen. *Z. Naturforsch.* **23b**, 316−319.
(26) Esterbauer, H. (1970) Kinetics of the reaction of sulfhydryl compounds with alpha-beta-unsaturated aldehydes in aqueous system. *Monatsh. Chem.* **101**, 782−810.
(27) Bories, G. F., Perdu-Durand, E. F., Sutra, J. F., and Tulliez, J. E. (1991) Evidence for glucuronidation and sulfation of zeranol and metabolites (taleranol and zearalanone) by rat and pig hepatic subfractions. *Drug. Metab. Dispos.* **19**, 140−143.
(28) Lowry, O. H., Rosebrough, N. H., Farr, A. G., and Randall, R. J. (1951) Protein measurement with the folin phenol reagent. *J. Biol. Chem.* **193**, 265−273.
(29) Bray, H. G., and James, S. P. (1960) The formation of mercapturic acids 4. Deacetylation of mercapturic acids by the rabbit, rat and guinea pig. *Biochem. J.* **74**, 394−397.
(30) Susuki, S., and Tateishi, M. (1981) Purification and characterization of a rat liver enzyme catalysing N-deacetylation of mercapturic acid conjugates. *Drug Metab. Dispos.* **9**, 573−577.
(31) Alary, J., Debrauwer, L., Fernandez, Y., Cravedi, J. P., Rao, D., and Bories, G. (1998) 1,4-Dihydroxynonene mercapturic acid, the major end metabolite of exogenous 4-hydroxy-2-nonenal, is a physiological component of rat and human urine. *Chem. Res. Toxicol.* **11**, 130−135.
(32) McIntyre, T. M., and Curthoys, N. P. (1960) The interorgan metabolism of glutathione. *Int. J. Biochem.* **12**, 545, 551.
(33) Hinchman, C. A., Matsumoto, H., Simmons, T. W., and Ballatori, N. (1991) Intrahepatic conversion of a glutathione conjugate to its mercapturic acid. Metabolism of 1-chloro-2,4-dinitrobenzene in isolated perfused rat and guinea pig livers. *J. Biol. Chem.* **266**, 22179−22185.
(34) Srivastava, S., Chandra, A., Bhatnagar, A., Srivastava, S. K., and Ansari, N. (1995) Lipid peroxidation product, 4-hydroxynonenal and its conjugate with GSH are excellent substrates of bovine lens aldose reductase. *Biochem. Biophys. Res. Commun.* **217**, 741−746.
(35) Srivastava, S., Liu, S. Q., Conklin, D. J., Zacarias, A., Srivastava, S. K., and Bhatnagar, A. (2001) Involvement of aldose reductase in the metabolism of atherogenic aldehydes. *Chem. Biol. Interact.* **130**−**132**, 563−571.
(36) Ramana, K. V., Dixit, B. L., Srivastava, S., Balendiran, G. K., Srivastava, S. K., and Bhatnagar, A. (2000) Selective recognition of glutathiolated aldehydes by aldose reductase. *Biochemistry* **39**, 12172−12180.
(37) Hers, H. G. (1960) L-Aldose-reductase. *Biochim. Biophys. Acta* **37**, 120−126.
(38) Srivastava, S., Ansari, N. H., Haiz, G. A., and Das, B. (1984) Aldose and aldehyde reductase in human tissues. *Biochem. Biophys. Res. Commun.* **217**, 741−746.
(39) Koh, Y. H., Park, Y. S., Takahashi, M., Suzuki, K., and Taniguchi, N. (2000) Aldehyde reductase gene expression by lipid peroxidation end products, MDA and HNE. *Free Radical Res.* **33**, 739−746.
(40) Burczynski, M. E., Sridhar, G. R., Palackal, N. T., and Penning, T. M. (2001) The reactive oxygen species- and Michael acceptor-inducible human aldo-keto reductase AKR1C1 reduces the α,β-unsaturated aldehyde 4-hydroxy-2-nonenal to 1,4-dihydroxy-2-nonene. *J. Biol. Chem.* **276**, 2890−2897.
(41) Chen, J., and Armstrong R. N. (1995) Stereoselective catalysis of a retro-Michael reaction by class mu glutathione transferases. Consequences for the internal distribution of products in the active site. *Chem. Res. Toxicol.* **8**, 580−585.
(42) Zhang, Y., Kolm, R. H., Mannervik, B., and Talalay, P. (1995) Reversible conjugation of isothiocyanates with glutathione catalysed by human glutathione transferases. *Biochem. Biophys. Res. Commun.* **206**, 748−755.
(43) Meyer, D. J., Crease, D. J., and Ketterer, B. (1995) Forward and reverse catalysis and product sequestration by human glutathione S-transferases in the reaction of GSH with dietary aralkyl isothiocyanates. *Biochem. J.* **306**, 565−569.
(44) Esterbauer, H., Zollner, H., and Scholz, N. (1975) Reaction of glutathione with conjugated carbonyls. *Z. Naturforsch.* **30c**, 466−473.
(45) Witz, G. (1989) Biological interactions of α,β-unsaturated aldehydes. *Free Radical Biol. Med.* **7**, 333−349.
(46) Baillie, T. A., and Slatter, J. G. (1991) Glutathione: a vehicle for the transport of chemically reactive metabolites in vivo. *Acc. Chem. Res.* **24**, 264−270.
(47) Eisenbrand, G., Schuhmacher, J., and Gölzer, P. (1995) The influence of glutathione and detoxifying enzymes on DNA damage induced by 2-alkenals in primary rat hepatocytes and human lymphoblastoid cells. *Chem. Res. Toxicol.* **8**, 40−46.

TX025671K